

# Adsorption of $\text{NO}_2$ on $\text{WSe}_2$ : DFT and photoelectron spectroscopy studies

R. Ovcharenko<sup>1</sup>, Yu. Dedkov<sup>2,‡</sup>, E. Voloshina<sup>1</sup>

<sup>1</sup> Humboldt-Universität zu Berlin, Institut für Chemie, 10099 Berlin, Germany

<sup>2</sup> SPECS Surface Nano Analysis GmbH, Voltastraße 5, 13355 Berlin, Germany

E-mail: elena.voloshina@hu-berlin.de

E-mail: dedkov@ihp-microelectronics.com

**Abstract.** The electronic structure modifications of  $\text{WSe}_2$  upon  $\text{NO}_2$ -adsorption at room and low temperatures were studied by means of photoelectron spectroscopy. We found only moderate changes in the electronic structure, which are manifested as an upward shift of the  $\text{WSe}_2$ -related bands to the smaller binding energies. The observed effects are modelled within the density functional theory approach, where a weak adsorption energy of gas molecules on the surface of  $\text{WSe}_2$  was deduced. The obtained experimental data are explained as a valence bands polarisation effect, which causes their energy shift depending on the adsorption geometry and the formed dipole moment.

‡ Present address: IHP, Im Technologiepark 25, 15236 Frankfurt (Oder), Germany

## 1. Introduction

Two dimensional materials, like graphene, *h*-BN, transition metal dichalcogenides (TMDs), etc., which have highest surface-to-volume ratio attract a lot of attention in the fundamental research as well as from the point of the possible technological applications [1–5]. For example, for graphene, the most promising ways to use its unique electronic structure (linear dispersion, zero band gap, and zero density of states at the Dirac point,  $E_D$ ) are utilization in flexible touch screens [6, 7] or gas sensors [8]. In the later work of Schedin *et al.* it was shown that the  $\mu\text{m}$ -sized graphene-based field-effect transistor shows unprecedented gas sensitivity even at room temperature. This functionality is explained by the change of the resistivity of the graphene sheet upon adsorption or desorption of molecules, which behave as donors or acceptors. The low density of states (DOS) in graphene around  $E_D$ , which in the neutral state coincides with the Fermi level ( $E_F$ ), allows easily tune the graphene conductivity upon very small charge transfer. Further, it was found that the sensitivity of such graphene-based gas sensors can be improved if dopants or defects are introduced in the graphene matrix [9–12].

Further search for the two-dimensional materials with tuneable transport properties leads to the experiments on the semiconducting transition metal dichalcogenides, with structural formula  $\text{MX}_2$ , where M is a metal atom (Mo or W) and X is a chalcogen (S or Se). These materials have a layered structure, where separated layers are bonded by weak dispersive forces. Each  $\text{MX}_2$ -layer consists of a metal atoms sandwiched between inert layers of chalcogen atoms as shown in Fig. 1(a,b). Covalent bonds localized between metal and chalcogen atoms lead to the semiconducting nature of these materials and to the inert nature of their surfaces at ambient conditions. However, it was shown that they are quite sensitive to the gaseous and higher temperature treatment. For example,  $\text{MoS}_2$  can be oxidized in the presence of oxygen or/and water already at 100°C [13, 14].

Recent demonstration of the field-effect transistor (FET) functionality for thin layers of  $\text{MoS}_2$  and other semiconducting TMDs [4, 5] brings the idea to use these materials in gas sensor devices. The  $\text{MoS}_2$ -based FET with a thickness of 2 – 4 single layers used for detection of gases demonstrated high sensitivity for

NO gas with a detection limit down to 0.8 ppm [15]. Here NO molecules behave as acceptors attracting the electron density from the  $\text{MoS}_2$  layer. Theoretical analysis of these data confirms the main findings [16]. In the same work the adsorption of other gases was also considered within the LSDA and GGA approaches and it was found that  $\text{H}_2$ ,  $\text{O}_2$ ,  $\text{H}_2\text{O}$ , NO, and  $\text{NO}_2$  adsorb weakly on  $\text{MoS}_2$  and behave like acceptors, whereas  $\text{NH}_3$  is a charge donor. These theoretical findings were later supported by the recent transport and gas sensing experiments [17].

Further developments in the field of electronics and optoelectronics of TMDs bring the W-based materials, like  $\text{WS}_2$  and  $\text{WSe}_2$ , in the forefront of these studies [18–20]. They have several advantages compared to  $\text{MoS}_2$ , since they have higher thermal stability as well as their electronic structure opens wide perspectives for applications in opto- and spin-electronics, and in the possible new field, the so-called valleytronics, where additional degree of freedom of the electron (valley polarization) might be used for the device operation. The gas sensing properties of  $\text{WS}_2$  were experimentally studied in Ref. [21], where the influence of the gas adsorption ( $\text{NH}_3$  and  $\text{O}_2$ ) on the photoelectrical properties of the transport devices was investigated at room temperature. Similar to the gas adsorption on  $\text{MoS}_2$ , it was found that molecules are physisorbed on the surface of  $\text{WS}_2$  with oxygen behaving as acceptor and ammonia leading to the *n*-doping of  $\text{WS}_2$ . With respect to the photoelectrical properties of  $\text{WS}_2$ , *p*- and *n*-doping of this material via molecules adsorption leads to reduction and to increase of photo-responsivity, respectively. Density-functional theory (DFT) analysis (without inclusion of the spin-orbit interaction) of the gas adsorption on  $\text{WS}_2$  [22] shows that the underlying band structure of TMD material is not influenced significantly upon molecules deposition confirming the weak interaction at the interface. In this work it was also found that adsorption of  $\text{O}_2$ , NO, and  $\text{NO}_2$  on  $\text{WSe}_2$  leads to the pinning of the lowest unoccupied molecular orbital around the Fermi level. It is interesting that no electronic structure studies by means of photoelectron spectroscopy (of the core levels or valence band states) of gas adsorption on TMDs were published in the literature, motivating the present studies.

Here we present X-ray and angle-resolved photoelectron spectroscopy (XPS and ARPES) results obtained during adsorption of  $\text{NO}_2$  on  $\text{WSe}_2(001)$ .

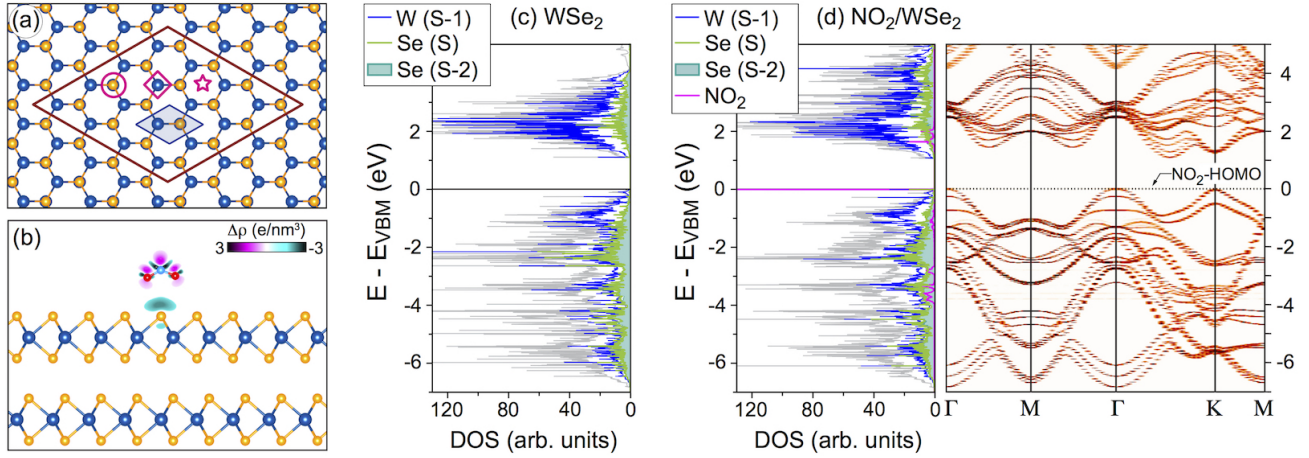


**Figure 1.** (a) Top view of WSe<sub>2</sub>. The corresponding (1 × 1) and (4 × 4) unit cells as well as the considered adsorption positions are marked in the figure. (b) Side view of the energetically most favourable NO<sub>2</sub>/WSe<sub>2</sub> structure is overlaid with the calculated difference electron density,  $\Delta\rho = \rho_{\text{NO}_2/\text{WSe}_2} - (\rho_{\text{WSe}_2} + \rho_{\text{NO}_2})$ . (c) Total (grey lines) and site-projected density of states calculated for the clean WSe<sub>2</sub>. (d) Total (grey lines) and site-projected density of states and band structure calculated for the NO<sub>2</sub>/WSe<sub>2</sub> system in its energetically most favourable adsorption structure shown in (b).

Small changes in the core-levels positions as well as in the valence band were found upon adsorption of gas molecules at room temperature and at 120 K indicating the physisorption nature of interaction at the gas-surface interface for TMD material. It is found that adsorption of NO<sub>2</sub> leads to the slight *p*-doping of WSe<sub>2</sub> as manifested by the rigid shift of core levels and valence band states of TMD to the smaller binding energies. These results are accompanied by the state-of-the-art DFT results, which give the small adsorption energy of NO<sub>2</sub> on WSe<sub>2</sub> of  $E_{\text{ads}} = 229$  meV/molecule. The theoretically obtained band structures confirm our experimental findings.

## 2. Methods

*Theory.* The DFT calculations were carried out using the projector augmented wave (PAW) method [23], a plane wave basis set and the generalized gradient approximation as parameterized by Perdew *et al.* [24], as implemented in the VASP program [25]. The plane wave kinetic energy cutoff was set to 500 eV. The spin-orbit correction, necessary for the proper description of the properties of WSe<sub>2</sub>, is taken into account via non-collinear magnetism as it is implemented in VASP. The long-range van der Waals (vdW) interactions were accounted for by means of the DFT-D2 approach [26]. The supercell used in this work has a (4 × 4) lateral periodicity with respect to WSe<sub>2</sub>. It is constructed from a slab of 3 layers of WSe<sub>2</sub> with a single NO<sub>2</sub> molecule adsorbed from one side and a vacuum region of approximately 20 Å. In the total energy calculations and during the structural relaxations the *k*-meshes for sampling the supercell Brillouin zone are chosen to be

as dense as 3 × 3 and 6 × 6, respectively, and centred at the  $\Gamma$ -point. The band structures calculated for the studied systems were unfolded to the WSe<sub>2</sub> (1 × 1) primitive unit cell according to the procedure described in Refs. [27, 28] with the code BandUP [28].

*Experiment.* The XPS and ARPES measurements with Al *K*α ( $h\nu = 1486.6$  eV) and He Iα radiation ( $h\nu = 21.2$  eV), respectively, were performed using a photoemission system with PHOIBOS 150 analyzer equipped with 2D-CCD detector. In this case a 5-axis motorized manipulator was used, allowing for a precise alignment of the sample in the *k* space for the ARPES experiments. The sample was azimuthally pre-aligned in such a way that the polar scans were performed along the  $\Gamma - \text{K}$  or  $\Gamma - \text{M}$  directions of the hexagonal Brillouin zone of WSe<sub>2</sub> with the photoemission intensity on the channelplate

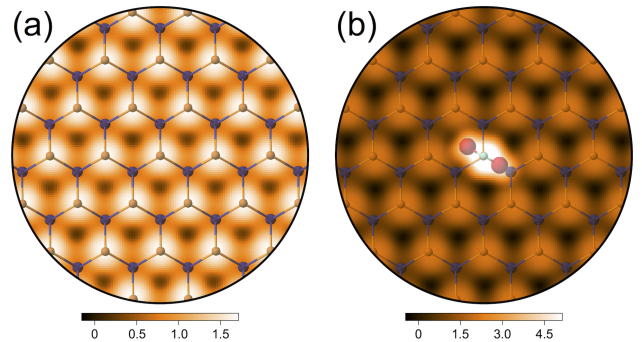


**Figure 2.** Calculated STM images of (a) WSe<sub>2</sub>(0001) and (b) NO<sub>2</sub>/WSe<sub>2</sub>(0001). Charge integration was performed in the energy range of 1 eV below the middle of the energy gap of WSe<sub>2</sub> (see Fig. 1). Corresponding height color scales (in Å) are shown in the lower parts.

images acquired along the direction perpendicular to the respective scanning direction. The final 3D data sets of the photoemission intensity as a function of kinetic energy and two emission angles,  $I(E_{kin}, angle_1, angle_2)$ , were then carefully analyzed. The base vacuum in the experimental station is in the range of  $1 \times 10^{-10}$  mbar.

WSe<sub>2</sub>(0001) samples (size of approximately  $2 \times 2 \times 0.2$  mm<sup>3</sup>) were pressed to the Mo sample holder with Ta clamps, which were used for the careful Fermi level calibration. Samples were cleaved in air and then were introduced in vacuum within the next 30 sec. Prior every series of XPS or ARPES experiments WSe<sub>2</sub> samples were carefully degassed at 300° C for 30 min. Dosing of NO<sub>2</sub> (measured in langmuir (L),  $1L = 1 \cdot 10^{-6}$  Torr  $\times$  1 sec) was performed via electronically controlled leak-valve and sample was kept either at room temperature or at 120 K.

### 3. Results and discussions

Adsorption of NO<sub>2</sub> molecules on the WSe<sub>2</sub>(0001) surface was studied within the DFT approach using PBE functional and dispersive forces (van der Waals) were taken into account via formalism proposed by Grimme [26]. Since the studied TMD material contains heavy elements, then the spin-orbit interaction was included in our calculations. Fig. 1(a,b) shows the top and side views of the crystallographic structure of WSe<sub>2</sub>, where high symmetry adsorption places for NO<sub>2</sub> are marked by the respective symbols. Our calculations for the NO<sub>2</sub>/WSe<sub>2</sub> system show that for all considered configurations the adsorption energy is in the range of 148 – 229 meV per NO<sub>2</sub>-molecule (see Fig. S1 and Table T1 in the Supplementary material where all configurations with adsorption energies are listed) placing this system to the class of weakly-bonded one, where adsorption is governed predominantly by the dispersion interaction. In our further analysis we will consider only one configuration, namely when NO<sub>2</sub> molecule is paced above Se (in the  $(4 \times 4)$  configuration resulting 0.06 ML coverage) where N-atom is located directly above Se-atom and both N-O bonds are directed downwards with one of them along the Se-W bond and other pointed to the centre of the W-Se “hexagon”. Taking into account the physisorption nature of the bonding in this system we can expect the similar results for other geometrical arrangement of NO<sub>2</sub> molecules on WSe<sub>2</sub>.

Figure 1(c) shows calculated total and atom-projected partial density of states (DOS and PDOS) of the studied systems as well as band structure obtained for the energetically most favourable NO<sub>2</sub>/WSe<sub>2</sub> structure. The calculated electronic structure for WSe<sub>2</sub> is in very good agreement with previously

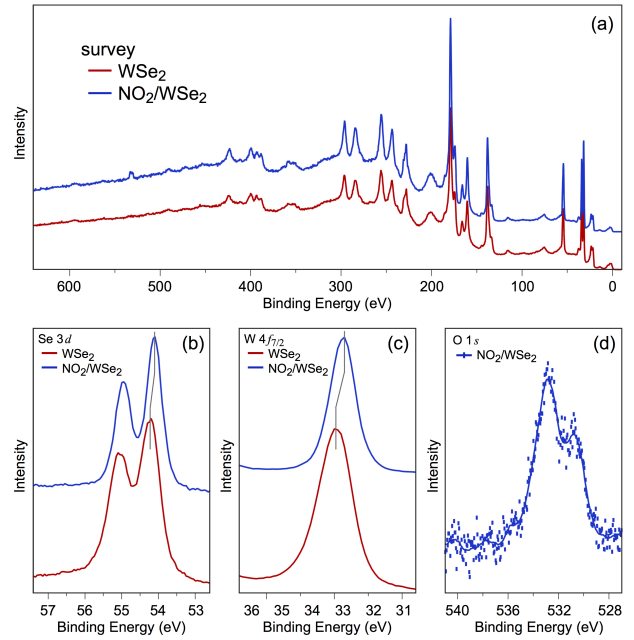


**Figure 3.** XPS spectra collected before (brown) and after (blue) adsorption of 600 L of NO<sub>2</sub> on WSe<sub>2</sub>: (a) survey, (b) Se 3d, (c) W 4f<sub>7/2</sub>, and (d) O 1s.

published theoretical and experimental data [29–33] as well as with our ARPES results presented later. Our calculations show that bulk WSe<sub>2</sub> is an indirect semiconducting material with a band gap of 1.1 eV. The obtained spin-orbit splitting at the *K*-point of the Brillouine zone is 485 meV.

Adsorption of NO<sub>2</sub> on the surface of WSe<sub>2</sub> leads to the formation of the impurity molecule-induced band in the vicinity of the top of the valence band of WSe<sub>2</sub>. Other NO<sub>2</sub>-related bands are found in the energy ranges at  $E - E_F \approx -3 \dots -4$  eV and  $E - E_F \approx 1.5 \dots 2$  eV. However, as one can see from the presented DOS and band structure of the NO<sub>2</sub>/WSe<sub>2</sub> system (Fig. 1(d)) there is no *hybridization* between valence band states of WSe<sub>2</sub>-substrate and molecular orbitals of NO<sub>2</sub>. Adsorption of NO<sub>2</sub> leads only to the charge transfer from substrate on the molecule as can be seen in Fig. 1(b), where charge depletion (accumulation) is found on Se-atoms (NO<sub>2</sub> molecules). Such effect leads to the polarization of the electronic states of substrate that can be detected in the photoemission experiments.

Weak adsorption of NO<sub>2</sub> on WSe<sub>2</sub>(0001) is also revealed in the calculated STM images (Fig. 2). In these calculations, performed in the framework of the Tersoff-Hamann formalism [34], the charge density integration was performed for the energy range of 1 eV below of the middle of the energy gap of WSe<sub>2</sub>. In this case the NO<sub>2</sub> HOMO state is included in the integration energy range for the NO<sub>2</sub>/WSe<sub>2</sub> system. One can see that adsorption of NO<sub>2</sub> on the surface of

the TMD material does not change the local density of states that can be taken as a signature of the absence of the orbital hybridization of the molecular orbitals and valence band states of  $\text{WSe}_2$ .

The behaviour of isolated  $\text{NO}_2$  molecule on  $\text{WSe}_2$  is similar to the one on the other TMD surfaces like  $\text{MoS}_2$  or  $\text{WS}_2$ . Indeed, in all cases the molecule-surface interaction is accounted for by weak dispersion forces, which do not drastically affect the electronic structure of adsorbent and result in relatively small adsorption energies: 229 meV, 412 meV [22], and 140 meV [17] for  $\text{WSe}_2$ ,  $\text{WS}_2$  and  $\text{MoS}_2$ , respectively. The adsorption geometry where oxygens of  $\text{NO}_2$  molecule are directed towards surface was found to be the most energetically favourable also for adsorption on the top of all these surfaces. However, the adsorption positions were found to be different: while for  $\text{WS}_2$  and  $\text{MoS}_2$  the molecule tends to adsorb above center of the ring, in  $\text{WSe}_2$  the site right above surface Se atom was found to be the most favourable. It should be noted here, the deviation in adsorption energies at different sites in the latter case is just about few meV that is, in principle, at the limit of DFT calculation precision. The important point is that in all cases  $\text{NO}_2$  acts as electron acceptor that helps to change the conductivity of surface upon  $\text{NO}_2$  adsorption in wide limits and opens up the potential opportunities to employ TMD materials as sensitive  $\text{NO}_2$  gas detector. During adsorption the surface valence electron occupies the LUMO of  $\text{NO}_2$  which finally turns out to be located around Fermi level of combined  $\text{NO}_2/\text{TMD}$  system. Such effect of the localisation of the flat adsorbate-induced impurity state at the Fermi level of TMD surface was early observed for a number of adsorbates like  $\text{O}_2$ ,  $\text{NO}$ ,  $\text{NO}_2$  on different TMD materials and was called Fermi-level pinning phenomenon [22]. As was shown in latter work such effect may be explained within traditional charge transfer theory provided isolated molecular LUMO is lower in energy than Fermi level of pristine surface. That causes the drift of electron density from the surface to unoccupied well-localised molecular orbital without hybridisation or formation of a strong chemical bonding between adsorbate and adsorbent allowing only weak dispersion electrostatic attraction.

In order to proof the theoretical findings on the weak adsorption of  $\text{NO}_2$  on  $\text{WSe}_2$  we perform systematic XPS and APRES experiments for this system. Experiments were performed with the  $\text{WSe}_2$  substrate kept either at 120 K or 300 K (RT). Fig. 3 shows (a) survey, (b)  $\text{Se } 3d$ , (c)  $\text{W } 4f_{7/2}$  XPS spectra of  $\text{WSe}_2$  before and after dosing of 600L of  $\text{NO}_2$  at 120 K. The  $\text{O } 1s$  XPS spectrum after dosing is shown in panel (d) (the  $\text{N } 1s$  emission line overlaps in energy with Se Auger lines). One can clearly see that adsorption of  $\text{NO}_2$  on  $\text{WSe}_2$  leads to the

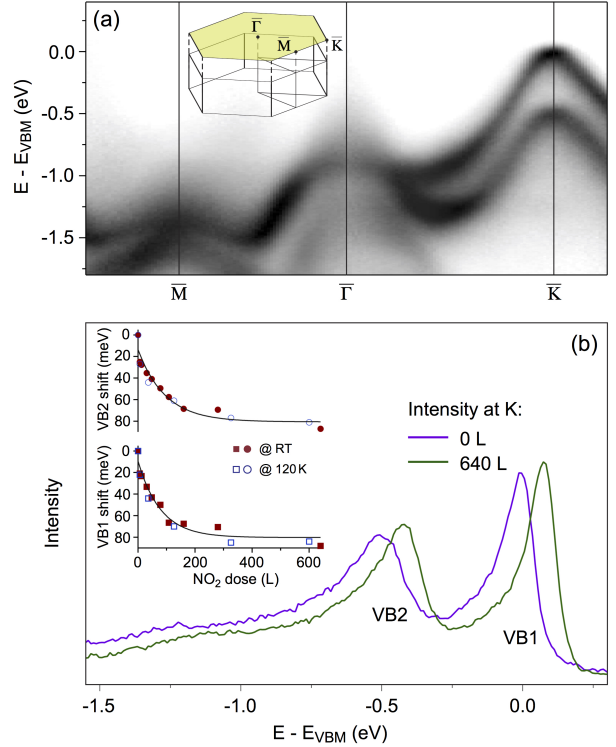


**Figure 4.** (a) Band structure of  $\text{WSe}_2$  along the high-symmetry directions of the hexagonal Brillouine zone (shown as an inset) extracted from the complete 3D data set for the ARPES intensity. (b) Intensity profiles extracted at the  $\bar{K}$ -point for the data collected before (pink) and after (green) adsorption of 640 L of  $\text{NO}_2$  on  $\text{WSe}_2$ . Insets show the respective energy shift of VB1 and VB2 as a function of  $\text{NO}_2$  dose. Two data sets are presented, which were collected at room temperature and 120 K.

minimal modifications of the TMD-related emission lines. The energy shift of  $\text{W } 4f$  and  $\text{Se } 3d$  lines of  $100 \pm 10$  meV to the smaller binding energies is detected indicating a weak interaction between adsorbed  $\text{NO}_2$  and underlying  $\text{WSe}_2$ . There are no additional low or high binding energy components in the respective XPS spectra pointing the absence of the strong chemical interaction in the system. As was discussed in the previous paragraph and can be concluded from the presented XPS data the interaction in the present adsorption system has vdW character that leads only to the polarization of the upper  $\text{WSe}_2$  layer due to the dipole moment of the adsorbed  $\text{NO}_2$  molecules. Such interaction is manifested as a rigid shift of all substrate-related emission lines to the lower binding energies.

The discussed effect of polarization of the top layer of TMD material was also detected in our ARPES experiments on  $\text{WSe}_2$  upon adsorption of  $\text{NO}_2$  molecules at RT and 120 K. Fig. 4(a) shows the ARPES photoemission map for clean  $\text{WSe}_2$  along the  $\bar{M} - \bar{\Gamma} - \bar{K}$  directions of the hexagonal Brillouine zone (shown as an inset) extracted from the complete 3D



data set acquired at 120 K. These data are in very good agreement with the band structure calculations presented earlier [Fig. 1(a)] and with previous data [32, 33]. The extracted value of spin-orbit splitting between two bands (marked as VB1 and VB2) at the  $\bar{K}$  point is 503 meV giving a very good agreement with the respective value obtained in the calculated band structure of WSe<sub>2</sub>.

Adsorption of NO<sub>2</sub> on WSe<sub>2</sub>(0001) surface leads to monotonic energy shift of the bands at the  $\bar{K}$  point as a function of the NO<sub>2</sub> and reaches the maximal value of  $87 \pm 5$  meV at 640 L of the NO<sub>2</sub> dose [Fig. 1(b)]. (For every NO<sub>2</sub> dose the Fermi level position was carefully calibrated via measurement of the PES spectra of the Ta clamps allowing to trace the shift of the valence band states of WSe<sub>2</sub>.) Here we would like to emphasise that the measured energy shift does not depend on the temperature of the WSe<sub>2</sub> substrate as can be seen from the presented dependencies of the energy positions of VB1 and VB2 bands as a function of the gas dose [inset of Fig. 1(b)]. Taking into account that energy shifts for the core-level lines and valence band states, measured by XPS and ARPES, respectively, have similar values we can conclude here on the weak physisorption of NO<sub>2</sub> molecules on WSe<sub>2</sub> leading to the polarization of the top layer of TMD substrate due to the dipole moment of NO<sub>2</sub> molecules. We can see that the studied surface of WSe<sub>2</sub> is extremely inert preventing further oxidation of the bulk of TMD material even at very high dose of the strong oxidation gas. This effect can be explained by the formation of the strong covalent-like bonds between W and Se in the layer, leading to the charge accumulation inside the layer and preventing any strong interactions on the surface. The presented experimental results are also supported by our DFT calculations which conclude on the weak interaction between NO<sub>2</sub> and WSe<sub>2</sub>.

#### 4. Conclusions

We present here the comprehensive study of the NO<sub>2</sub> adsorption on the WSe<sub>2</sub> surface by means of a number experimental spectroscopic techniques like XPS and ARPES supported by accurate spin-polarised DFT-D2 electronic structure calculations. At each step our theoretical and experimental results are in well agreement with each other that indicates in reasonable theoretical model and experimental conditions. Experimentally, the weak physisorption of NO<sub>2</sub> molecules on WSe<sub>2</sub> leading to the polarization of the top layer of TMD substrate due to the dipole moment of NO<sub>2</sub> molecules has been found. These findings were then confirmed by means of DFT calculation showing us the absence of any hybridisation between NO<sub>2</sub> molecular orbitals with WSe<sub>2</sub> bands and

filling of the NO<sub>2</sub> LUMO with surface electron density. The latter effect, which is also closely related to the so-called Fermi-level pinning phenomenon, may be easily explained within traditional charge transfer theory and has been early observed for adsorption of the O<sub>2</sub>, NO and NO<sub>2</sub> molecules on the top of different TMD surfaces.

#### Acknowledgements

The High Performance Computing Network of Northern Germany (HLRN-III) is acknowledged for computer time. Financial support from the German Research Foundation (DFG) through the grant VO1711/3-1 within the Priority Programme 1459 “Graphene” is appreciated.

#### References

- [1] Geim A K and Novoselov K S 2007 *Nature Mater.* **6** 183–191
- [2] Castro Neto A, Guinea F, Peres N, Novoselov K and Geim A 2009 *Rev. Mod. Phys.* **81** 109–162
- [3] Geim A 2009 *Science* **324** 1530–1534
- [4] Radisavljevic B, Radenovic A, Brivio J, Giacometti V and Kis A 2011 *Nature Nanotech.* **6** 147
- [5] Wang Q H, Kalantar-zadeh K, Kis A, Coleman J N and Strano M S 2012 *Nature Nanotech.* **7** 699–712
- [6] Bae S, Kim H, Lee Y, Xu X, Park J S, Zheng Y, Balakrishnan J, Lei T, Kim H R, Song Y I, Kim Y J, Kim K S, Ozyilmaz B, Ahn J H, Hong B H and Iijima S 2010 *Nature Nanotech.* **5** 574–578
- [7] Ryu J, Kim Y, Won D, Kim N, Park J S, Lee E K, Cho D, Cho S P, Kim S J, Ryu G H, Shin H A S, Lee Z, Hong B H and Cho S 2014 *ACS Nano* **8** 950–956
- [8] Schedin F, Geim A K, Morozov S V, Hill E W, Blake P, Katsnelson M I and Novoselov K S 2007 *Nature Mater.* **6** 652–655
- [9] Zhang Y H, Zhou K G, Xie K F, Zeng J, Zhang H L and Peng Y 2010 *Nanotechnology* **21** 065201
- [10] Kumar B, Min K, Bashirzadeh M, Farimani A B, Bae M H, Estrada D, Kim Y D, Yasaei P, Park Y D, Pop E, Aluru N R and Salehi-Khojin A 2013 *Nano Lett.* **13** 1962–1968
- [11] Jiang Y, Yang S, Li S, Liu W and Zhao Y 2015 *J. Nanomater.* **2015** 504103
- [12] Lee G, Yang G, Cho A, Han J W and Kim J 2015 *Phys. Chem. Chem. Phys.*; doi: 10.1039/C5CP04422G
- [13] Ross S and Sussman A 1955 *J. Phys. Chem.* **59** 889–892
- [14] KC S, Longo R C, Wallace R M and Cho K 2015 *J. Appl. Phys.* **117** 135301
- [15] Li H, Yin Z, He Q, Li H, Huang X, Lu G, Fam D W H, Tok A I Y, Zhang Q and Zhang H 2011 *Small* **8** 63–67
- [16] Yue Q, Shao Z, Chang S and Li J 2013 *Nanoscale Res. Lett.* **8** 425
- [17] Cho B, Hahm M G, Choi M, Yoon J, Kim A R, Lee Y J, Park S G, Kwon J D, Kim C S, Song M, Jeong Y, Nam K S, Lee S, Yoo T J, Kang C G, Lee B H, Ko H C, Ajayan P M and Kim D H 2015 *Sci. Rep.* **5** 8052
- [18] Bhimanapati G R, Lin Z, Meunier V, Jung Y, Cha J, Das S, Xiao D, Son Y, Strano M S, Cooper V R, Liang L, Louie S G, Ringe E, Zhou W, Kim S S, Naik R R, Sumpter B G, Terrones H, Xia F, Wang Y, Zhu J, Akinwande D, Alem N, Schuller J A, Schaak R E, Terrones M and Robinson J A 2015 *ACS Nano* **9** 11509–11539
- [19] Gmitra M and Fabian J 2015 *Phys. Rev. B* **92** 155403–6

- [20] Withers F, Del Pozo-Zamudio O, Mishchenko A, Rooney A P, Gholinia A, Watanabe K, Taniguchi T, Haigh S J, Geim A K, Tartakovskii A I and Novoselov K S 2015 *Nature Mater.* **14** 301–306
- [21] Huo N, Yang S, Wei Z, Li S S, Xia J B and Li J 2014 *Sci. Rep.* **4** 5209
- [22] Zhou C, Yang W and Zhu H 2015 *J. Chem. Phys.* **142** 214704–9
- [23] Blöchl P E 1994 *Phys. Rev. B* **50** 17953–17979
- [24] Perdew J, Burke K and Ernzerhof M 1996 *Phys. Rev. Lett.* **77** 3865–3868
- [25] Kresse G and Hafner J 1994 *J. Phys.: Condens. Matter* **6** 8245–8257
- [26] Grimme S 2006 *J. Comput. Chem.* **27** 1787–1799
- [27] Popescu V and Zunger A 2012 *Phys. Rev. B* **85** 085201
- [28] Medeiros P V C, Stafström S and Björk J 2014 *Phys. Rev. B* **89** 041407
- [29] Finteis T, Hengsberger M, Straub T, Fauth K, Claessen R, Auer P, Steiner P, Hufner S, Blaha P and Vögt M 1997 *Phys. Rev. B* **55** 10400
- [30] Jiang H 2012 *J. Phys. Chem. C* **116** 7664–7671
- [31] Yuan H 2013 *Nature Phys.* **9** 563–569
- [32] Riley J M, Mazzola F, Dendzik M, Michiardi M, Takayama T, Bawden L, Granerød C, Leandersson M, Balasubramanian T, Hoesch M, Kim T K, Takagi H, Meevasana W, Hofmann P, Bahrany M S, Wells J W and King P D C 2014 *Nature Phys.* **10** 835–839
- [33] Le D, Barinov A, Preciado E, Isarraraz M, Tanabe I, Komesu T, Troha C, Bartels L, Rahman T S and Dowben P A 2015 *J. Phys.: Condens. Matter* 182201
- [34] Tersoff J and Hamann D R 1985 *Phys. Rev. B* **31** 805–813

Supplementary material for the manuscript:

**Adsorption of NO<sub>2</sub> on WSe<sub>2</sub>: DFT and photoelectron spectroscopy studies**

R. Ovcharenko<sup>1</sup>, Yu. Dedkov<sup>2</sup>, and E. Voloshina<sup>1</sup>

<sup>1</sup> Humboldt Universität zu Berlin, Institut für Chemie,  
12489 Berlin, Germany

<sup>2</sup>SPECS Surface Nano Analysis GmbH, Voltastraße 5,  
13355 Berlin, Germany

E-mail: elena.voloshina@hu-berlin.de

E-mail: dedkov@ihp-microelectronics.com

**Content:**

1. Table T1: Calculated adsorption energies of the NO<sub>2</sub>/WSe<sub>2</sub> system.
2. Figure S1: Considered adsorption geometries of the NO<sub>2</sub>/WSe<sub>2</sub> system.



**Table S1.** Calculated adsorption energies (in meV) of the NO<sub>2</sub> molecule on the WSe<sub>2</sub> surface for geometries shown in Figure S1.

	<b>geom-1</b>	<b>geom-2</b>	<b>geom-3</b>
<b>Ring</b>	-160	-223	-153
<b>Se</b>	-148	-229	-147
<b>W</b>	-155	-224	-149

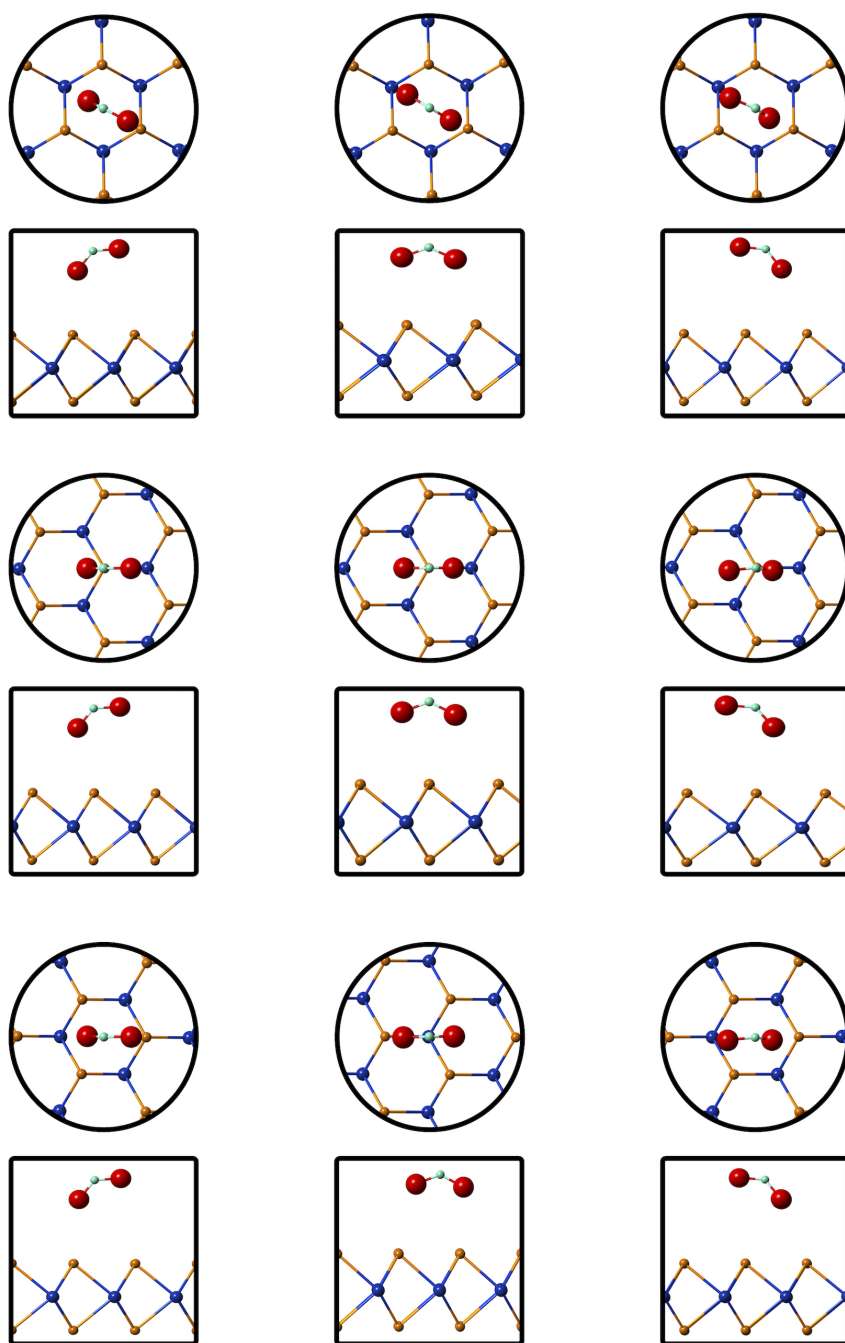


**Figure 5. Figure S1.** Adsorption geometries of the NO<sub>2</sub>/WSe<sub>2</sub> system after ionic relaxation. In total we have considered three adsorption places: above the ring (top), above Se atom (middle) and above W atom (bottom) lines. For each place three molecule orientations were taken into account: one molecule oxygen is directed towards surface and center of the ring (geom-1 – left), both molecule oxygens are directed towards surface (geom-2 – middle) and one molecule oxygen is directed towards one of the surface site (geom-3 – right) columns.